Thermoresponsive Toughening in LCST-Type Hydrogels with Opposite Topology: From Structure to Fracture Properties

Hui Guo, Cécile Mussault, Annie Brûlet, Alba Marcellan, Dominique Hourdet, Nicolas Sanson

Thermo-responsive Toughening in LCST-type Hydrogels with Opposite Topology: From Structure to Fracture Properties

Hui Guo,[†,‡] *Cécile Mussault,*[†,‡] *Annie Brûlet,*[§] *Alba Marcellan,*[*,†,‡] *Dominique Hourdet,*[*,†,‡] *and Nicolas Sanson*[*,†,‡]

[†]École Supérieure de Physique et de Chimie Industrielles de la Ville de Paris (ESPCI), ParisTech, PSL Research University, Sciences et Ingénierie de la Matière Molle, CNRS UMR 7615, 10 rue Vauquelin, F-75231, Paris cedex 05, France.

[‡]Sorbonne-Universités, UPMC Univ Paris 06, SIMM, 10 rue Vauquelin, F-75231 Paris cedex 05, France.

[§]Laboratoire Léon Brillouin (UMR 12 CEA CNRS), CEA Saclay, F-91191 Gif-sur-Yvette Cedex, France.

Email addresses:

alba.marcellan@espci.fr , dominique.hourdet@espci.fr, nicolas.sanson@espci.fr

ABSTRACT

The challenge of this work was to investigate the role of topology in LCST hydrogels that strongly and reversibly thermo-reinforce their mechanical strength under isochoric conditions. To achieve this, two different hydrogels with opposite topologies were designed on the basis of grafted architectures using equal amounts of water-soluble chains (poly(*N*,*N*-dimethylacrylamide) = PDMA) and LCST polymer chains (poly(*N*-isopropylacrylamide) = PNIPA). By working under isochoric conditions, with almost 85 wt% of water in the whole temperature range (20 to 60 °C), we were able to clearly highlight the impact of the phase transition of PNIPA on the mechanical reinforcement of the gel without any interference of the volume transition. These graft hydrogels, designed with PNIPA in the backbone (GPN-D) or as pendant chains (GPD-N), have been studied more specifically by tensile tests and 2D neutron scattering at rest and under deformation. From these complementary techniques, we show that PNIPA side-chains in GPD-N self assemble above their transition temperature into a micellar network greatly interfering with the covalent PDMA frame. While the elastic modulus increases reversibly more than ten times throughout the phase transition, other properties like elongation at break and fracture resistance are greatly enhanced with temperature. At high temperature and under extension, SANS data highlight the affine deformation of PNIPA domains. By comparison, the opposite topology with PNIPA forming the cross-linked backbone undergoes a similar phase separation with temperature and gives rise to a bicontinuous structure that aligns under loading. The collapsed phase being topologically defined as the load bearing phase, GPN-D displays remarkable fracture toughening with crack bifurcation at high temperature whereas GPD-N gels fracture in a more conventional way.

Keywords: poly(*N*-isopropylacrylamide), hydrogels, nanostructure, responsive toughening, crack bifurcation.

INTRODUCTION

During the last decades, covalent hydrogels have received considerable attention due to their important potential as biological containers or mechanical transducers. They are actually used

in many bio-applications[1-4] such as superabsorbents, contact lenses, drug delivery systems or scaffolds for tissue engineering but they intrinsically suffer from their poor mechanical strength. More recently, new challenges have emerged in this field such as the reinforcement of the mechanical properties in order to elaborate smart and innovative polymer-based materials. On one hand, one can find original covalent architectures like double networks,[5] slide-ring gels[6] or tetra-PEG gels,[7] which have been shown to strongly improve the mechanical properties in terms of stiffness, fracture toughness or stretchability. On the other hand, a more versatile approach consists in introducing physical interactions into the covalent network. In this case, the reinforcement of mechanical properties has been nicely demonstrated with nanocomposite[8] and hybrid networks,[9] which develop reversible interactions between the polymer matrix and inorganic nanofillers like clay platelets or silica nanoparticles. In these examples, hybrid hydrogels showed improved mechanical response with an increase of modulus, dissipation and fracture properties. This idea to mix both reversible and covalent cross-links within the same structure to get tough hydrogels has been extended afterwards to other physical interactions. We can mention for instance hydrophobically modified hydrogels,[10-12] which show a large increase of their extensibility and resistance to crack propagation due to a “costly” deformation of hydrophobic associations under stress, or other mixed systems involving complex formation like calcium alginates embedded in a cross-linked polyacrylamide network[13] or polyampholyte hydrogels.[14] With these examples, it is clearly shown that the mechanical behavior of hydrogels can be dramatically reinforced by introducing secondary interactions in the covalent structure, but in these architectures the transient character of the physical network cannot be finely and reversibly tuned using simple environmental triggers.

Now, from a fundamental point of view, as well as for specific applications, it could be interesting to switch on/off the association process in response to environmental triggers.

Moreover, such systems would offer the possibility to investigate the exact contribution of physical interactions to the mechanical properties of the swollen network and/or to develop hydrogels with responsive toughness. In order to tackle this problem, one can immediately think about *stimuli* responsive polymers that are currently used as transducers in smart polymeric systems. In this regard, a physical trigger like temperature is very appealing and thermo-responsive polymers obviously appear as a natural choice of building blocks to prepare polymer networks with responsive mechanical properties. During the last three decades, thermo-responsive polymers have been widely investigated as they provide technological answers for industrial or medical applications that require materials or complex fluids with improved or responsive properties above/below a given temperature. However, since the pioneering work of Tanaka et al.[15] describing the volume phase transition of responsive hydrogels, most of academic studies on responsive polymer networks were dedicated to the swelling/deswelling behavior of hydrogels in order to develop smart systems able to respond reversibly under external *stimuli*. Even for hybrid systems which demonstrate excellent mechanical properties, like nanocomposite gels based on poly(*N*-isopropylacrylamide) (PNIPA), almost all the studies were carried out at low temperature, in the swollen state. The main issue when crossing the transition threshold is that in most cases the polymer network concurrently undergoes a large volume transition that dominates the macroscopic properties. It is then difficult to draw a direct comparison of the mechanical behavior before, during and after the transition in order to achieve a complete understanding of the structure/properties relationships. In this framework, we have to mention the pioneering work of Shibayama et al.[16] that have reported a large increase of dynamic storage modulus in PNIPA hydrogels under isochoric conditions when crossing the transition temperature. However, this study was mainly focused on low deformation properties of isolated PNIPA-based networks in their collapsed state with consequently a low water content. Recently,

Gong et al.[17] have expanded this concept of gel toughening induced by phase separation using polyacrylamide (PAM) gels collapsed in water/dimethylformamide mixtures. In this study, the comparison between phase separated PAM gels and homogeneous samples, studied at the same polymer concentration, clearly demonstrates the consequence of the formation of a highly concentrated segregated phase, mostly glassy in this case, upon the improvement of the mechanical behavior. Nevertheless, the polymer concentration in the gel was again very high (more than 40 %) and the liquid medium was almost organic in this case. Clearly, if one wants to take benefit of the phase separation in gels to improve the mechanical behavior, while keeping a reasonable level of swelling, it is important to reconsider the primary structure and the topology of the network. To the best of our knowledge, there are only a couple of papers where the authors have tried to reduce the volume phase transition in PNIPA-based hydrogels by adjusting the hydrophilic/hydrophobic balance of the network. Nevertheless, while they succeeded on this point, the mechanical properties were not strongly modified by the phase transition.[18, 19]

By exploring original topologies of covalently cross-linked gels, we have recently demonstrated[20] the remarkable asset represented by the phase-separation process on the fracture properties of PNIPA network grafted with hydrophilic side-chains. Beyond the excellent fatigue resistance, self-healing and high fracture energies, phase-separated gels studied under isochoric conditions highlighted a thermo-toughening with systematic crack bifurcation, unreported so far in gels. The impact of polymer topology seems to be crucial as also preliminary reported on thermo-responsive grafted copolymers on self-assembling and rheological properties in aqueous solutions.[21] The main objective of the present project was to investigate more systematically the structure/properties relationships of thermo-responsive hydrogels under isochoric conditions and more especially on the effect of network topology. To achieve this goal, the “LCST/hydrophilic” balance was set with equal amounts of LCST

and water-soluble polymers; namely poly(*N*-isopropylacrylamide) (PNIPA) and poly(*N*,*N*-dimethylacrylamide) (PDMA). Working with fixed polymer concentrations and PNIPA/PDMA ratio, the impact of the network topology has been addressed by preparing two grafted networks designed with opposite topologies (see **Figure 1)**.

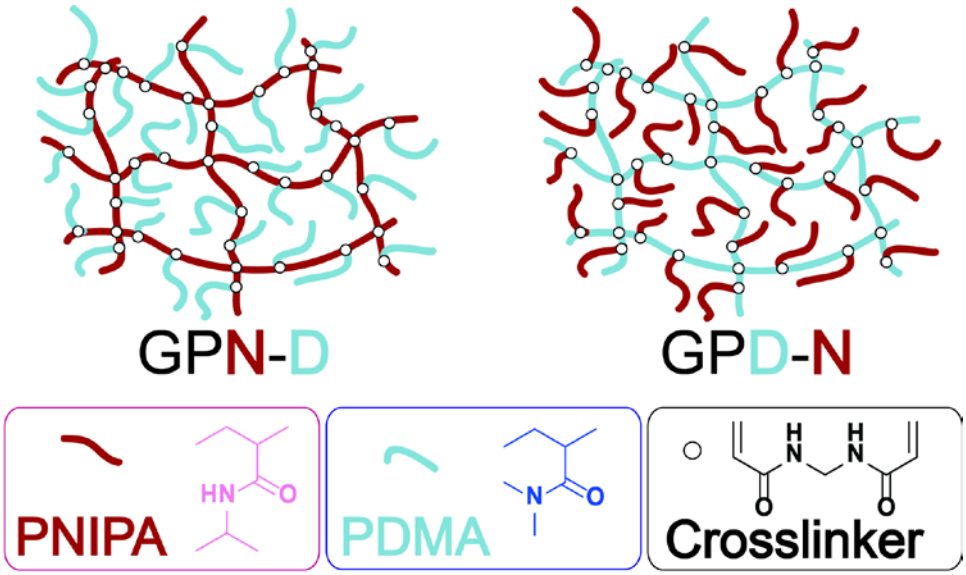

Figure 1. Schematic primary structure of thermo-responsive grafted hydrogels GPN-D (**left**) and GPD-N (**right**) exhibiting opposite topologies.

GPD-N is a hydrophilic PDMA network (referred as GPD) grafted with thermo-responsive PNIPA side-chains (denoted as -N), while GPN-D has the exact inverse topology with a thermo-responsive PNIPA network (denoted as GPN) grafted with hydrophilic PDMA side-chains (denoted as -D).

The structure and macroscopic properties of these hydrogels have been investigated as a function of temperature by classical characterization methods like swelling experiments, Differential Scanning Calorimetry, and rheology, and more specifically by tensile tests and 2D small angle neutron scattering performed at rest and under deformation. This comprehensive set of analyses clearly highlights that under isochoric conditions, the phase

161 separation of PNIPA is responsible for a strong and reversible mechanical reinforcement of
162 hydrogels with a large impact of the topology.
163

164 **EXPERIMENTAL SECTION**

165 **Materials**

166 *N*-isopropylacrylamide (NIPA, Aldrich), *N*,*N*-dimethylacrylamide (DMA, Aldrich),
167 cysteamine hydrochloride (AET·HCl, Fluka), potassium peroxodisulfate (KPS, Aldrich),
168 acrylic acid (AA, anhydrous > 99%, Fluka), dicyclohexylcarbodiimide (DCCI, Aldrich), *N*,*N*'-
169 methylenebisacrylamide (MBA, Aldrich) and tetramethylethylenediamine (TEMED, Aldrich)
170 were used as received. All organic solvents were analytical grade and water was purified with
171 a Millipore system combining inverse osmosis membrane (Milli RO) and ion exchange resins
172 (Milli Q) for synthesis and purification.

173 **Synthesis of polymer precursors**

174 The synthesis of PDMA and PNIPA macromonomers was performed as previously
175 described[20, 21] using a telomerization process with cysteamine hydrochloride followed by
176 modification of the amino end-group with acrylic acid in order to get the vinyl function. The
177 absolute characterization of macromonomers by size exclusion chromatography gives similar
178 average molar masses for the two polymers: M_n=36 kg/mol (Đ=1.4) for PNIPA and M_n=39
179 kg/mol (Đ=1.3) for PDMA. These polymerizable precursors are used afterwards to prepare
180 graft copolymer networks.

181 **Synthesis of hydrogels**

182 The same procedure was followed to prepare both grafted networks. Monomer, cross-linker
183 (stock solution of MBA) and macromonomer were initially dissolved in a given amount of

water under nitrogen bubbling; the temperature of the reactor being controlled with an ice bath. Stock solutions of KPS and TEMED were separately prepared under nitrogen atmosphere and after 30 min aliquots were added into the reaction medium. After fast mixing (2 min), the final formulation was rapidly transferred between glass plates of 2 mm width under nitrogen atmosphere and the reaction was left to proceed overnight in the fridge (4 °C). The resulting hydrogels were then cut with a die-cutter of rectangular or round shape and directly used for DSC and swelling experiments or stored into paraffin oil before mechanical testing in order to avoid any change in hydrogel composition induced by swelling or drying. For both topologies, the weight ratio “monomer/macromonomer/water” was constant, equal to 1/1/10, and the molar ratio “monomer/MBA/KPS/TEMED” was set equal to 100/0.1/1/1. The details are reported in **Table 1**.

Table 1 Formulation of thermo-responsive grafted hydrogels

	Monomer g	MBA mg	Macromonomer g	M_n kg/mol	Đ	KPS mg	TEMED mg	Water g
GPN-D	1	1.36	1	39	1.3	23.9	10.3	10
GPD-N	1	1.56	1	36	1.4	27.3	11.7	10

Gel composition and swelling experiments

The swelling degree of the gel, Q, was defined as the weight ratio of the hydrated gel over the dried gel. Samples, originally in their preparation state (Q_0=6), were weighted and placed at a given temperature in a large excess of pure water. Water was changed every day and the swelling was determined with time until equilibrium (Q_e) was reached.

Differential Scanning Calorimetry (DSC)

The phase transition of PNIPA-based hydrogels was investigated by Differential Scanning Calorimetry using a DSC Q200 from TA instrument. Gel samples (around 80 mg), equilibrated with a reference filled with the same quantity of solvent, were submitted to temperature cycles between 10 and 70 °C. The heating and cooling rates were fixed at 2 °C/min.

Rheology

The viscoelastic properties of hydrogels in their preparation state (discs with 4 cm diameter and 2 mm thickness) were studied using a stress-controlled rheometer (AR 1000 from TA Instruments) equipped with a plate/plate geometry (diameter 40 mm). The experiments were performed in the linear regime and the temperature was controlled by a high power Peltier system. The experimental conditions were fixed at constant frequency (1 Hz) and shear stress (2 Pa). A particular care was taken to avoid the drying of the sample by using a homemade cover which prevents from water evaporation during experiment. In these conditions, dynamic moduli (G' and G'') were recorded between 20 and 70 °C by applying heating and cooling scans of 0.5 °C/min.

Large strain mechanical behavior: tensile, cycling, fracture and shape-memory properties.

Tensile tests were performed on a standard tensile Instron machine, model 5565, equipped with an environmental chamber especially designed for the study and allowing for a precise control of the swelling state. The device used a 10 N load cell (with a relative uncertainty of 0.16 % in the range from 0 to 0.1 N) and a video extensometer which follows the local displacement up to 120 mm (with a relative uncertainty of 0.1 % at full scale).

The gel samples are cut with a punch and their final dimensions are L_0 = 30 mm, w_0 = 4.9 mm and t_0 = 2 mm. The gauge length was taken constant (L ≅ 20 mm). For high temperature or long-term experiments, in order to prevent the samples from evaporation, tests were conducted in an environmental chamber consisting of a temperature controlled paraffin oil bath surrounding the sample. As a control experiment we verified the total immiscibility of the paraffin oil with the gel within the temperature range investigated in this study.

All tensile experiments were carried out at a strain rate of 0.06 s^{-1}, which corresponds to an initial velocity of 1.2 mm/s, with at least three tests per sample to check the reproducibility. During the test, time (t), force (F) and displacement (L) were recorded while the nominal stress ($\sigma=F/S_0$), the strain ($\varepsilon=(L-L_0)/L_0$) and stretch ratio λ ($\lambda=L/L_0$) were calculated.

Loading-unloading experiments were performed in order to characterize the recovery processes. Measurements were carried out on hydrogels of similar size, using the same conditions as described previously at 60 °C. First, the loading process was performed with given deformation and a waiting gap of 3 min was applied before unloading to initial deformation. Between cycles, a waiting gap of another 3 min was applied for the recovery.

Fracture energy data were obtained using the single edge notch geometry. A notch of about 1 mm length was made in the middle of the sample strip, whose total width was 5 mm. The fracture energy (G_C) was calculated using the following expression:[22] $G_C=(6.W.c)/\sqrt{\lambda_c}$ **,** with c the length of the initial notch, $\lambda_c=L_c/L_0$ the deformation rate at break in single edge notch experiment and W the strain energy density calculated by integration of the stress versus engineering strain of un-notched samples, until ε_c ($\varepsilon_c=\lambda_c-1$).

The shape-memory properties were investigated by first stretching the gel to a certain nominal stretch ratio at 20 °C, and then immersing it at 60 °C during 3 minutes. Gel was then unloaded (i.e. at zero external force) by removing the clamps. The gels were kept waiting at 60 °C for 6

minutes. Strain recovery was followed by cooling down the gel at 20 °C for another 6 minutes. The gel length was measured overtime.

Small Angle Neutron Scattering (SANS)

SANS experiments were performed at Laboratoire Léon Brillouin (CEA-Saclay, France) on the PAXY spectrometer dedicated to anisotropic measurements. Two experimental configurations at the sample-to-detector distance D=2.5 and 4.7 m, with respective incident neutron wavelengths of λ_0 = 4.5 and 12 Å, provide a scattering vector modulus $q = (4\pi/\lambda_0)\sin(\theta/2)$ ranging between 3.10^{-3} and 5.10^{-1} $Å^{-1}$ (where θ is the scattering angle). For SANS experiments, gel plates of 2-mm thick were specially synthesized in D_2O to intensify the scattering contrast between the polymer network and the solvent.

For isotropic analyses, the gel discs (diameter = 14 mm and thickness = 2 mm) punched from plate samples in their preparation state were fit inside a ring spacer hermetically sandwiched between two quartz slides. The gel samples were then placed in a temperature controlled autosampler and let to equilibrate at least during 30 min at a given temperature (between 15 and 60 °C) prior to scattering experiments.

For anisotropic measurements performed with hydrogels under uni-axial deformation, a special device has been developed as described in a previous paper (see **Figure S1** in Supporting information).[23] With this setup, the hydrogel strip, immersed into the thermostated chamber filled with perfluorodecalin, can be studied for hours without any risk of drying. In the following, all the anisotropic scattering experiments have been carried out during at least 1 hour for each sample in a given deformation state. For all the analyses, the efficiency of the detector cell was normalized by the intensity delivered by a pure water cell of 1-mm thickness and absolute measurements of the scattering intensity I(q) (cm^{-1} or 10^{-8} $Å^{-1}$) were obtained from the direct determination of the incident neutron flux and the cell solid angle. Finally, the

coherent scattering intensity of the gel was obtained after subtracting the contribution of the solvent used, as well as perfluorodecalin for samples studied in the oil environment. For 2D SANS experiments, the incident neutron flux recorded on a two dimensional detector built up with 15500 cells of 25 mm^2, is directly transformed into a 2D image with a color code. After sector averaging (see details in supporting information), the data have been quantitatively analyzed in terms of diffusion pattern.

RESULTS AND DISCUSSION

Transition temperature and swelling behavior

As illustrated in **Figure 2a**, both gels feature an endothermic peak upon heating which is related to the overall energy balance of hydrogen bonds disruption/re-formation between amide groups and water molecules. The phase transition of graft hydrogels occurs more readily when PNIPA is located in the backbone instead of the side-chains, as already observed with linear graft copolymers,[21] and the endothermic process starts at about 30 °C for GPN-D; almost 2-3 °C below the transition of GPD-N. Upon heating, PNIPA chains have to balance two opposite and competing effects: the enthalpic contribution, due to intra-molecular hydrogen bonds and hydrophobic interactions that stabilizes the globular conformation, and the entropic elasticity that goes against the coil-globule transition.

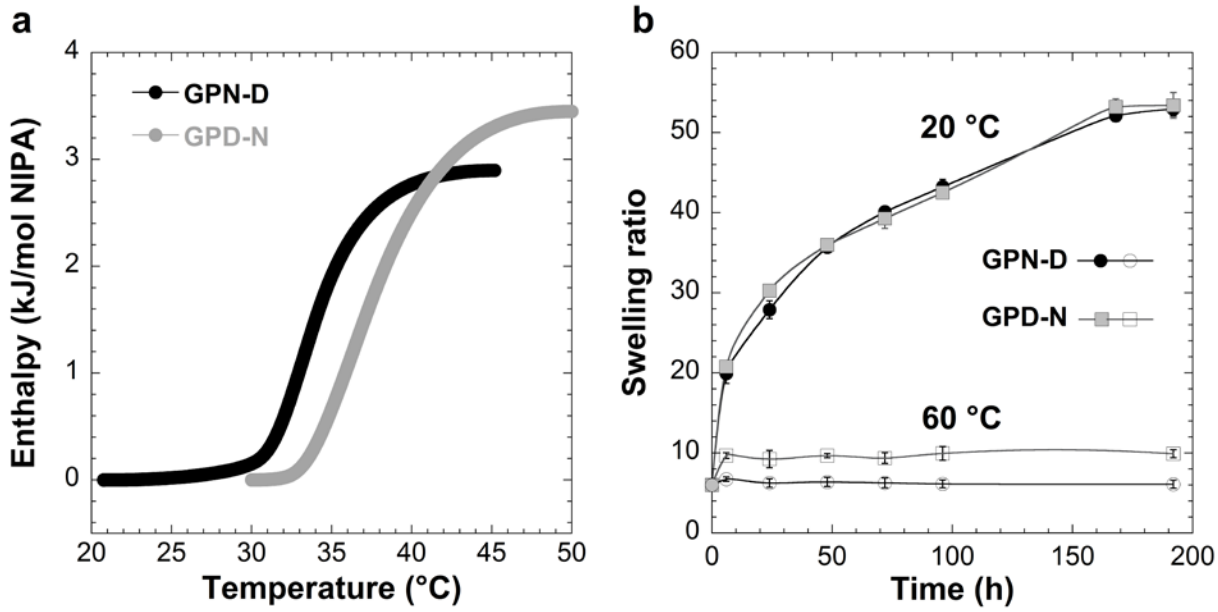

Figure 2. a) Thermograms of GPN-D (black) and GPD-N (grey) hydrogels (heating rate=2 °C/min). **b)** Swelling behavior of GPN-D (●○)and GPD-N (■□) hydrogels in pure water at 20 (filled symbols) and 60 °C (empty symbols).

Above the critical temperature, the polymer-polymer attractions prevail, and the resulting collapse and aggregation of macromolecular chains are generally accompanied by a large volume phase transition of the macroscopic network. Nevertheless, it is well known that the level of deswelling strongly depends on the hydrophobic/hydrophilic balance of the macromolecular structure. As shown in **Figure 2b**, the introduction of hydrophilic PDMA chains inside the copolymer network improves the macroscopic volume stability of GPD-N and GPN-D, especially at high temperature. In these experiments, the swelling properties were determined well below (20 °C) and far above (60 °C) the transition temperature previously determined by DSC. At low temperature, both hydrogels swell similarly with time and reach their equilibrium after one week at about $Q_e \cong 53$; well above the initial swelling corresponding to the preparation state ($Q_0=6$). No significant difference is observed between the two hydrogels and this is quite reasonable if we take into account that GPN-D and GPD-N

have been prepared with the same PNIPA, PDMA, MBA and water concentrations and if we assume that at 20 °C PNIPA and PDMA have similar hydrophilicity. At high temperature (60 °C), the swelling at equilibrium remains a little higher than the initial swelling preparation state. The higher value obtained for GPD-N (Q_e=10) compared to GPN-D (Q_e=6.1) emphasizes the impact of topology on the volume transition with a lower efficiency for swelling when the LCST polymer belongs to the cross-linked backbone. These swelling experiments point out that, if the gel samples are isolated from water environment and kept in their preparation state, they will be able to retain their initial swelling (Q_0=6) and consequently their initial volume over the whole range of temperatures, i.e. well below and above the phase transition. Obviously, these isochoric conditions obtained for GPD-N and GPN-D hydrogels with a relatively high water content (almost 85 wt%) are the result of a prospective work based on various hydrogel samples prepared by either changing the PNIPA/PDMA ratio or their relative concentrations during the synthesis.

Phase-separated structure at rest and linear viscoelasticity response

Both hydrogels with opposite topologies, GPN-D and GPD-N, were studied by small angle neutron scattering (SANS) in order to investigate the nanostructure of the polymer network as a function of the temperature, first in static mode.

As confirmed in a previous study,[21] the replacement of H_2O with D_2O does not induce significant modification of the transition temperature in linear graft copolymers PNIPA/PDMA. Therefore, all the gel samples have been studied in pure D_2O in order to enhance the scattering contrast arising from the phase separation. The results are presented in **Figure 3**.

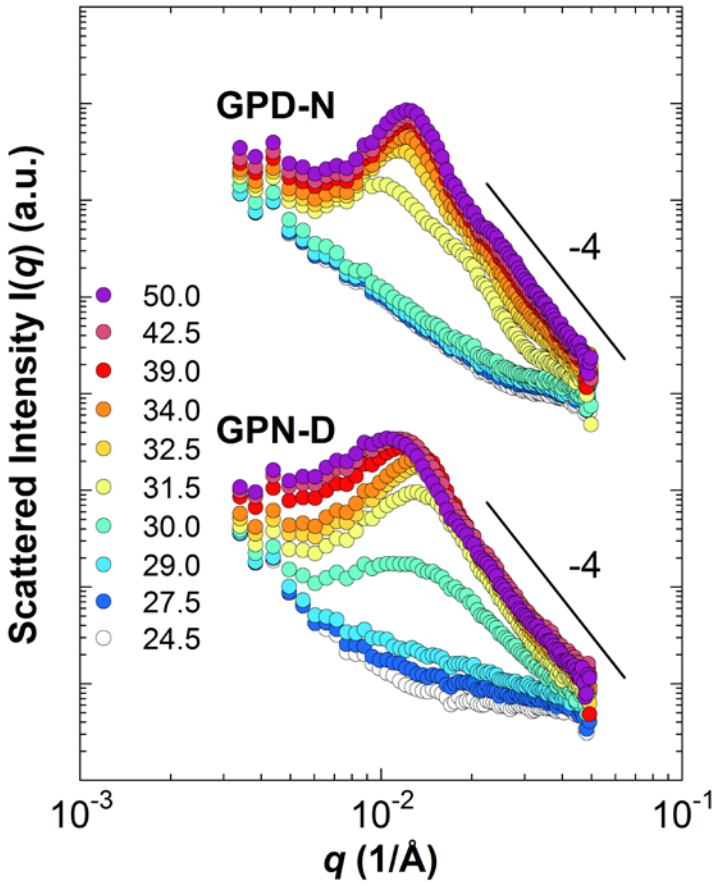

Figure 3. Scattered intensities in log-log scale of GPD-N (up) and GPN-D (down) hydrogels prepared in D_2O as a function of temperature. The intensities have been shifted for clarity.

329

330 From a general point of view, the SANS data obtained with the gels are qualitatively very
331 similar to those already described for weakly charged PNIPA gels[24] and recently reported for
332 homologous linear graft copolymers.[21] For both hydrogels, the scattered intensity dramatically
333 increases during the heating process on the whole *q*-range investigated. As observed from
334 DSC, the transition temperature starts around 30 °C for GPN-D and above 31 °C for GPD-N
335 in agreement with the departure of the phase transition of PNIPA chains forming the
336 backbone or the side-chains, respectively. This phase transition of PNIPA chains induces an
337 increase of the scattered intensity over the whole *q*-range with the appearance of a correlation
338 peak at low *q* value, typically between *q*=0.01 and 0.02 $Å^{-1}$, figuring fluctuation

concentrations between rich- and poor-PNIPA phases. We also observe that the correlation peak is narrower for GPD-N, compared to GPN-D, in relation with a better ordered biphasic structure when the phase transition arises from the side-chains rather than the backbone. At high temperature, the scattered intensity of both hydrogels decays in the high-q regime with the same Porod law $I(q) \sim q^{-4}$, characteristic of a sharp interface. Moreover, **Figures 3** clearly shows that the position of the correlation peak, q_{peak}, varies differently during the phase transition for both hydrogels and their respective evolutions are highlighted in **Figure 4**.

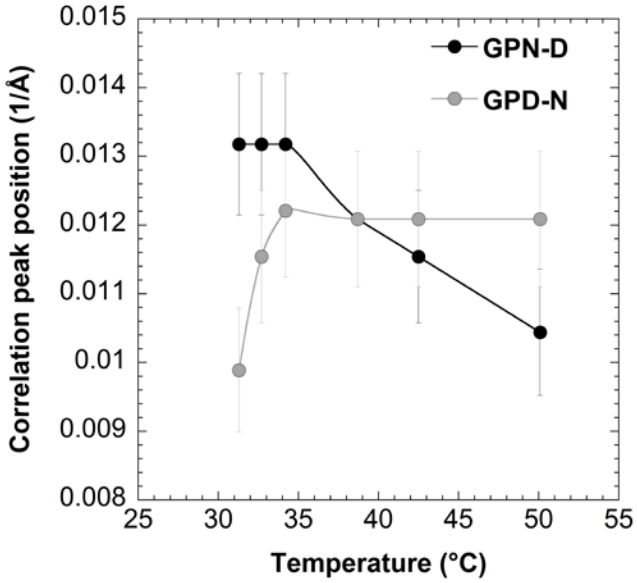

Figure 4. Evolution of the correlation peak position for both hydrogels as a function of the temperature.

In the case of GPN-D, the position of the correlation peak, q_{peak}=0.0132 Å^{-1}, corresponding to a characteristic distance ($d_c=2\pi/q_{peak}$) of 480 Å, is rather constant between 31 and 34 °C; i.e. just above the transition threshold. At higher temperatures, the position of q_{peak} subsequently shifts to lower q values, indicating larger fluctuations with further development of the microphase separation. On the other hand, the wavelength of the correlation peak in GPD-N gradually increases at the beginning of the phase separation, below 34 °C, and finally remains constant up to 50 °C (q_{peak} = 0.012 Å^{-1}; $d_c \cong$ 520 Å), indicative of a maintained microphase-separated structure for GPD-N.

Beside this qualitative description, a more quantitative analysis can be done by using adequate models for both hydrogels. For that purpose, we start from the fact that above the transition temperature SANS curves demonstrate the existence of a two-phase system with a characteristic wavelength (correlation peak) and a sharp interface as deduced from the asymptotic regime. Moreover, we assume here that GPD-N forms a more regular and stable structure with PNIPA-rich domains dispersed into the PDMA network. This assumption, which is consistent with SANS data reported for analogous graft copolymers,[21] comes from the relatively narrow mid-width of the correlation peak observed in **Figure 3** as well as the presence of weak additional oscillations at 0.0226 and 0.0341 $Å^{-1}$. For GPD-N, we assume that a fraction of PNIPA side-chains (f_{PNIPA}) self-assemble at a given temperature, above the transition, into polydisperse spherical domains (with R_2, σ, N_{agg} and ϕ_{PNIPA}: the core radius, the standard deviation of the Gaussian size distribution, the number of PNIPA chains inside the micelle and the volume fraction of PNIPA inside the core) which behave with a repulsive hard sphere potential of radius R_{HS}. In this micellar model (core-shell with hard sphere repulsions), R_{HS} is higher than R_2 in order to take into account the surrounding PDMA chains (see inset in **Figure 5a**). For the microphase separation of GPN-D, the continuous phase being topologically defined by the PNIPA network, we assume the formation of a bicontinuous structure between PNIPA-rich domains and PDMA/water phase and apply the Teubner-Strey model. This phenomenological model was originally introduced to represent the micellar structure of ternary systems: water/oil/surfactant mixtures.[25] Since then, it is widely used to describe random bicontinuous structures in microemulsions. This model assumes a pair correlation function of the form:

$$\gamma(r) = \frac{d}{2\pi r} exp\left(-\frac{r}{\xi}\right) sin\left(\frac{2\pi r}{d}\right) \qquad \{eq.1\}$$

with ξ a correlation length (length beyond which correlations die out) and d the typical length scale of the structure (see inset in **Figure 5b**), characteristic of a domain size or periodicity and roughly equal to $d_c=2\pi/q_{peak}$. The analytical description of these two models is given in supporting information.

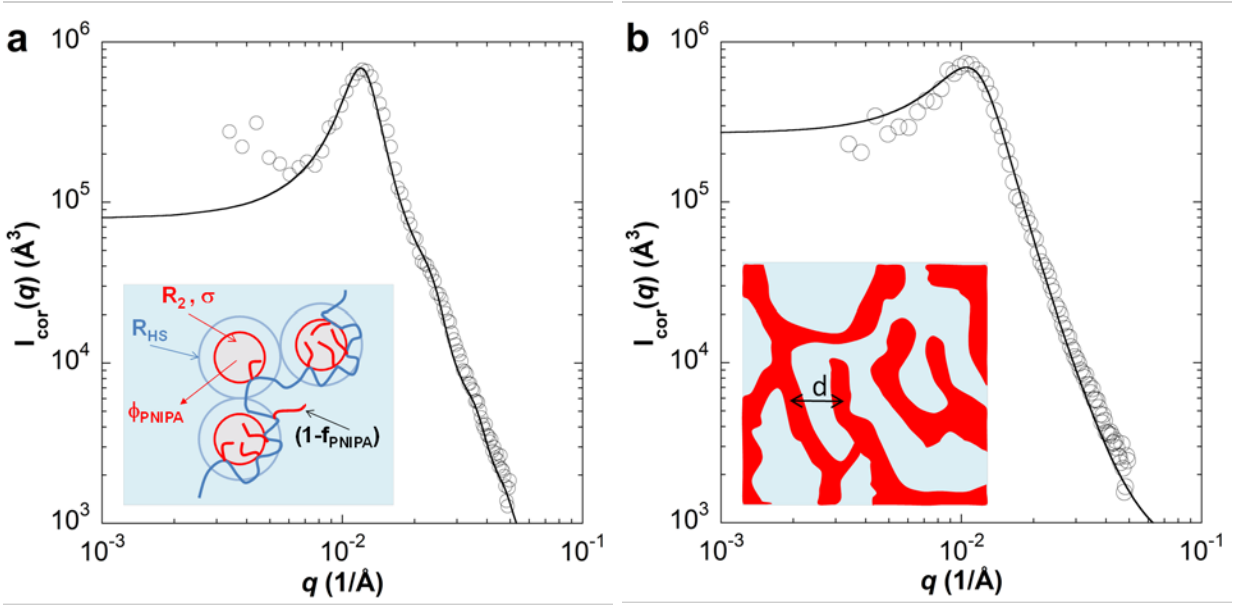

Figure 5. Normalized scattered intensity profiles of **a)** GPD-N and **b)** GPN-D at 50 °C. Solid lines represent fits according to the two applied models. The insets correspond to the models: Micellar model for GPD-N with R_2, the radius of the micellar core, σ the standard deviation of the Gaussian size distribution, N_{agg} the number of PNIPA chains inside the micelle core, R_{HS} the hard sphere radius, ϕ_{PNIPA}, the volume fraction of PNIPA inside the core, and (1-f_{PNIPA}), the fraction of non aggregated PNIPA chains. Teubner-Strey model (TS) based on a bicontinuous system with average periodicity d.

An example of model fitting is shown in **Figure 5** in the case of scattering data obtained at high temperature (50 °C) and the fitting parameters determined at all temperatures above the phase transition are reported in **Tables 2** and **3**.

In the case of GPD-N, the micellar model fits reasonably well the experimental data without any adjusting parameter in the whole *q*-range, except the small upturn observed at low *q* value in relation with interactions at larger scales. According to this model, PNIPA side-chains are assumed to self-associate into polydisperse spherical domains surrounded by a PDMA shell which characteristic size remains almost constant above T_c (R_2 = 160 Å and R_{HS} = 260 Å), as well as its polydispersity that can be defined by $\sigma/R_2 = 0.28$. In the same temperature range, the main variations come from the increasing number of PNIPA side chains embedded into these domains (f_{PNIPA} = 0.3 to 0.75) and from their increasing concentration inside the micellar core (ϕ_{PNIPA} = 0.5 to 0.77). At 50 °C, 75 % of PNIPA chains are involved in the formation of micro-domains and their volume fraction inside the core is about 77 %. In these conditions, the level of the phase separation defined by $f_{PNIPA}*\phi_{PNIPA}$ is about 0.6 and close to the values already reported for analogous graft copolymers.[21]

Table 2. Fitting parameters obtained for GPD-N at different temperatures using the core-shell model with hard sphere repulsions.

Temperature (°C)	R_2 (Å)	σ (Å)	R_{HS} (Å)	f_{PNIPA}	ϕ_{PNIPA}	ϕ_{HS}	N_{agg}
31.3	---	---	---	0.3*	0.5*	0.21*	158*
32.7	160	45	260	0.5	0.57	0.31	180
34.2	160	45	260	0.6	0.6	0.36	190
38.7	160	45	260	0.7	0.68	0.37	215
42.5	160	45	260	0.75	0.72	0.37	227
50.1	160	45	260	0.75	0.77	0.35	243

**Approximate values*

In the case of GPN-D, the Teubner-Strey model fits also quite well the experimental data over the whole *q*-range for all temperatures above 31 °C. As the temperature increases, we observe that the periodicity, d, continuously increases above 34 °C while the correlation length, ξ,

does not evidence clear variation in this range, mainly because of a larger standard deviation for this parameter (**Table 3**).

Table 3. Fitting parameters obtained for GPN-D at different temperatures using the Teubner-Strey model.

Temperature (°C)	d (Å)	ξ (Å)	$\xi_{S/V}$ (Å)
31.3	440	248	202
32.7	446	278	237
34.2	452	279	245
38.7	490	277	253
42.5	521	264	262
50.1	565	261	268

According to Teubner and Strey, the correlation lengths can also be calculated from the total interfacial area (S_2) as:[26] $\xi_{S/V} = a\phi_1\phi_2(S_2/V)$ with ϕ_2 and ϕ_1 =1-ϕ_2, the volume fraction of each phase (here 2 refers to the PNIPA-rich phase); S/V, the total specific area of the internal interface (see the details in supporting information) and *a*, a numerical value taken equal to 7.16 used for a large variety of bicontinuous emulsions.[26] As shown in **Table 3**, these calculated values ($\xi_{S/V}$) are similar in magnitude from those extracted from the TS model but they display a regular increase with increasing temperature, underlining the increasing size of PNIPA domains in GPN-D gels contrary to GPD-N where their size remain constant .

Such a drastic change of the gel structure induced by the phase-separation of PNIPA is expected to drive concurrently large modifications of the macroscopic properties. The absence of volume transition when heating the gels from their preparation state fully satisfied the isochoric conditions and a first investigation of the linear viscoelastic properties was carried out by dynamic rheology. The results reported in **Figure 6** with both gel samples, demonstrate that the collapse of PNIPA segments that occurs at the molecular level is capable of inducing large modifications of the elastic properties, even in the absence of volume transition. When

PNIPA chains are under the coil state, for $T<<T_c$, the shear elastic moduli are slightly the same for both topologies as expected from their similar syntheses, grafted architectures and solvent affinity. Interestingly, for $T>>T_c$, although the micro-phase separated structure varies with the gel topology, GPN-D and GPD-N continue to display very similar viscoelastic responses with temperature. At 60 °C, viscoelastic behaviors (G' and G") are almost similar for the two hydrogels with a relatively low contribution of viscoelastic losses (G"/G' ≅ 0.1).

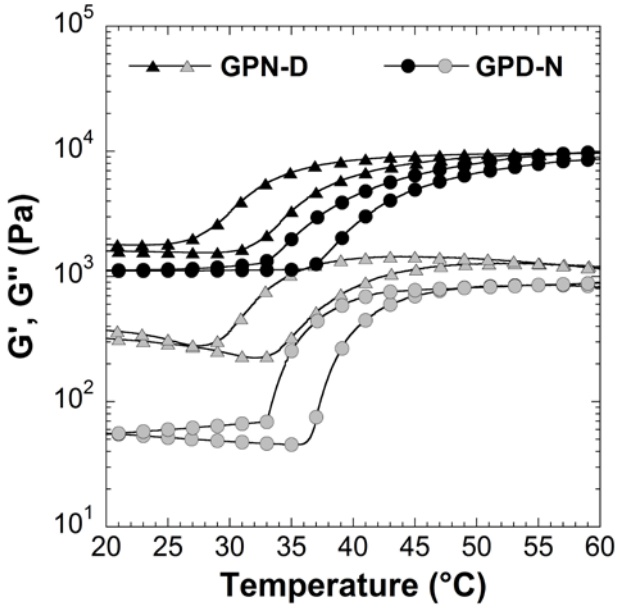

Figure 6. Temperature dependence of viscoelastic properties at 1 Hz of GPD-N (circles) and GPN-D (triangles) hydrogels at preparation state with a heating/cooling rate of 0.5 °C/min. Black symbols stand for G' and grey symbols for G".

Note that the variation of the viscoelastic properties is totally reversible and the same values of G', around 1 and 10 kPa, are obtained at low and high temperatures respectively even after several heating/cooling cycles. This result is in good agreement with the fact that the gel does not change its volume during the phase transition as water would be irreversibly expelled from the rheometer during heating in the opposite case. On the other hand, depending of the heating/cooling rate, a strong symmetric hysteresis can be observed between heating and

cooling cycles. This hysteresis can be highly reduced from almost ΔT=30 to 5 °C by simply decreasing the scanning rate respectively from 10 to 0.5 °C/min (see **Figure S2** in Supporting information). Thermal hysteresis has been widely reported in the literature from DSC experiments performed on PNIPA gels.[27] It is generally observed that the rate of cooling strongly impacts the transition temperature due to the slow relaxation of the frozen network. On the other hand the rate of heating is expected to have little influence on the onset of the phase separation since the segregation between PNIPA-rich and water-rich regions is very prompt compared to the characteristic times involved in the reorganization of the polymer-rich and solvent-rich interfaces featured by a diffusion coefficient typical of the glassy state.[27] Here, as shown in **Figure S2**, the hysteresis signature is very symmetric on both sides of the transition temperature determined by DSC. The main reason for this artifact can be related to the relatively high gap used with the plate/plate geometry (2 mm for gels instead of 56 µm for solutions with cone/plate geometry) that does not allow reaching instantaneous thermal equilibrium in the whole discoid sample.

Large strain behavior: structure and mechanical properties.

SANS is widely used to analyze the structure of polymer networks under deformation as thermal fluctuations of polymer chains and more especially frozen inhomogeneities give rise to very informative anisotropic patterns.[25, 28-31] Working with hydrogels, deformation can be induced by swelling experiments which emphasize their structural inhomogeneities or more simply by mechanical stretching. Here, the complex spatial distribution of strains and stresses in deformed hydrogels is a crucial issue for understanding the reinforcement mechanisms.[23, 32] As the dynamics of PNIPA-rich domains greatly slow down at high temperature forming some quenched heterogeneities, these scatterers can be used as probes to follow their average displacement under mechanical deformation and to investigate the local nanostructure of thermo-responsive hydrogels. For that purpose, a series of SANS experiments have been

carried out on GPN-D and GPD-N hydrogels, under incremental elongation ratio, from $\lambda = 1$ to 3-5 at 60 °C, i.e. well above the phase transition temperature. The 2D SANS spectra are reported in **Figures 7a** and **7d**, for GPD-N and GPN-D respectively, and for comparison, their corresponding monotonic tensile behavior after thermal equilibrium at 20 and 60 °C are shown in **Figure 7b**. At 20 °C, below the phase transition, both topologies demonstrate the classical response of a polymer network that is dominated by entropic elasticity, with an initial tensile modulus around 4 kPa in agreement with dynamic experiments. On the other hand, at 60 °C, well above the transition temperature, the stress-strain mechanical response highlights the formation of PNIPA-rich domains that strongly enhances the stiffness of the mechanical response (i.e. the initial modulus is increased by one order of magnitude), independently of the gels topologies. Interestingly, both stiffness and elongation at break are simultaneously enhanced. Thus work of extension, defined by the area under the tensile curve increased from 11 to 149 $kJ.m^{-3}$ and 30 to 288 $kJ.m^{-3}$, respectively for GPD-N and GPN-D. From these results, thermo-toughening is clearly demonstrated and the GPN-D topology appears to be more efficient. Note that as previously observed with the dynamic analysis performed within the linear regime, the large strain behaviors of both topologies are surprisingly perfectly superimposed.

From a structural point of view (**Figures 7a** and **7d**), both unstrained samples ($\lambda = 1$), GPN-D and GPD-N, display at 60 °C an isotropic pattern with a circular diffraction ring corresponding to the correlation peak of the structure factor discussed in the previous section (**Figure 3**). At intermediate deformation ($\lambda = 1.75$), the pattern of GPD-N changes to a rather uniform elliptically shaped correlation band qualitatively showing that PNIPA microdomains move apart in the stretching direction while they get closer in the perpendicular direction due to the transverse compression.

483

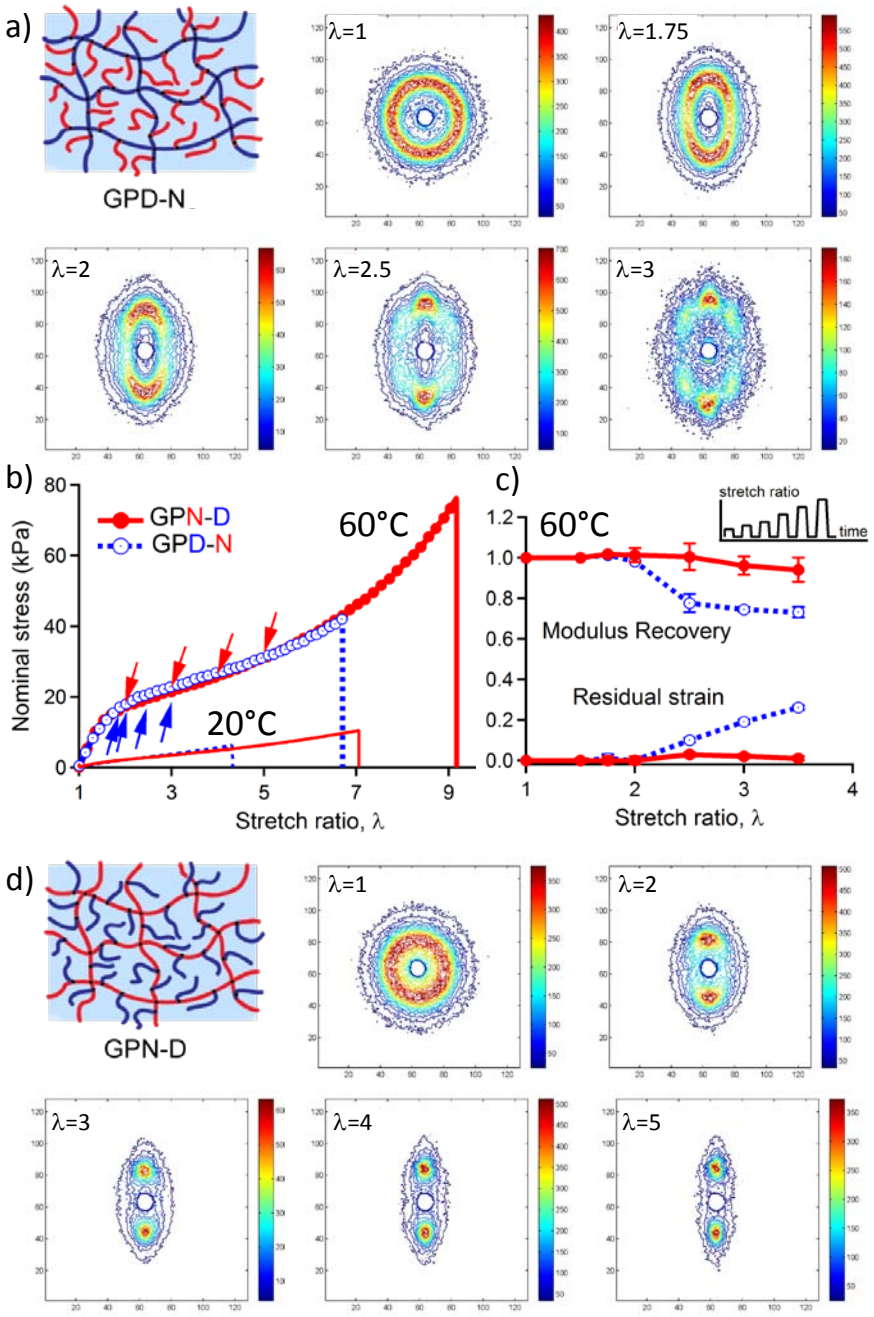

Figure 7. Structure and properties of GPD-N and GPN-D under deformation. **a)** and **d)** Primary structure of GPD-N and GPN-D, respectively, along with their iso-intensity SANS patterns obtained after a step-by-step loading at 60 °C. The direction of the uni-axial deformation is along the horizontal axis. **b)** Uni-axial tensile stress-strain curves of GPN-D (red continuous line) and GPD-N (blue dashed line) hydrogels at 20 and 60 °C. The arrows refer to the elongation ratio studied by SANS. **c)** Modulus recovery and

residual strain at 60 °C for GPN-D (red continuous line) and GPD-N (blue dashed line) after a series of loading/unloading steps up to different maximal stretch ratio.

484

485 At higher deformation the 2D spectrum turns to a non-uniform azimuthal intensity
486 distribution, effectively showing up diffraction arcs and then spots for $\lambda \geq 2$ in the
487 perpendicular direction. At a macroscopic scale (**Figure 7c**) this threshold value of applied
488 stretch ratio corresponds to the initiation of irreversible processes, suggesting damage
489 phenomenon within the network. Indeed, for $\lambda>2$ the mechanical behavior of GPD-N exhibits
490 a loss in modulus recovery with residual strain, at least within the time of experiment. At very
491 high deformation (λ = 2.5-3), four additional spots are clearly observed for azimuthal angles μ
492 around 60, 120, 240 and 300°; μ being defined as μ=0° in the stretching direction. These four
493 new spots highlight some reorganization within the microstructure which can have different
494 origins. For instance, this has been observed with micellar gels of triblock copolymers by
495 Reynders and co-workers.[33] Depending on the block composition and solvent concentration,
496 they show that under stretching the initial hexagonal arrangement of polystyrene (PS) micellar
497 cores undergo either affine deformation or improved angular as well as spatial order,
498 indicating the formation of well defined layers of regularly spaced PS domains in the
499 perpendicular direction of stretching. Diffraction patterns combining these two extreme cases
500 have been obtained with different micellar systems. It is worth noting that the development of
501 a similar 4 spot-patterns has been reported under stretching with a lot of hybrid materials like
502 silica particles in dry polyacrylate latex films,[34] polyisoprene/silica[35] and nanocomposite or
503 nano-hybrid hydrogels.[22, 32, 36] This morphological modification observed under stretching
504 originates from the transverse compression that pushes the particles towards each other and
505 from the localized shear displacements of these particles avoiding each other when they are in
506 close contact. The main difference with hydrogels reinforced with inorganic nanoparticles is

that in our system the microdomains are deformable under stretching. In this case, another possible scenario would be that at low relative deformation (below λ=2) the spherical microdomains are distorted into prolate ellipsoid with their major axis along the equatorial direction. In this case the PNIPA-rich domains become closer in the perpendicular direction and farther along the deformation axis. At higher level of deformation, above some critical stress, the prolate microdomain becomes unstable and undergoes disruption processes. In this case, the formation of additional scatterers would be responsible for the emergence of new diffraction spots.

By comparison, the isotropic circular pattern of GPN-D rapidly turns into an elliptically shaped correlation band with a non-uniform azimuthal intensity distribution with two diffraction spots above λ =2 in the perpendicular direction. Note that in this case, the behavior is highly recoverable, up to λ=4: the GPN-D topology is capable to maintain 94 % of its initial modulus and residual strain is negligible after 3 minutes at rest. At higher deformation (λ=3-5), the anisotropy becomes even more important with the same spots always centered at about the same position. Qualitatively, this means that the inter-domains distance in GPN-D is more or less preserved in the perpendicular direction during the process of domain deformation upon stretching. Taking into account the values of q_{peak} determined in the parallel- and perpendicular-directions at each deformation, the ratio $R = q_{peak,\lambda=1}/q_{peak,\lambda}$ allows to correlate the local displacement with the macroscopic deformation of the gel ($\lambda = L/L_0$). As shown in **Figure 8**, the local deformation in GPD-N is rather affine with the macroscopic deformation in both parallel (//) and perpendicular ($\perp$) directions, at least up to λ =2 along the deformation axis and up to λ =3, the largest deformation applied to this sample, in the perpendicular direction.

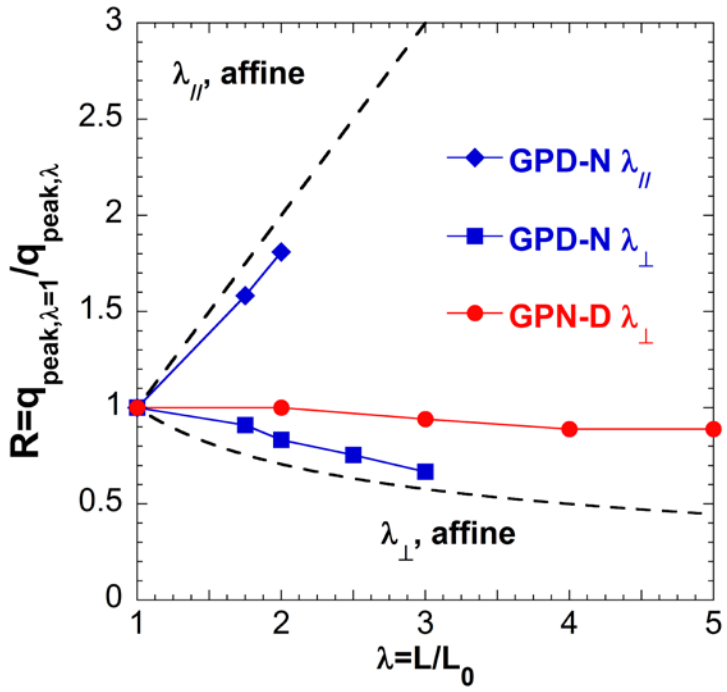

Figure 8.

Comparison between the macroscopic affine deformation of hydrogel samples, along parallel- (//) and perpendicular-axis (⊥), and the local deformation probed through the scattering peak ratio: R = $q_{peak,\lambda=1}$ / $q_{peak,\lambda}$

By contrast, the behavior of GPN-D is not affine at all as the correlation peak rapidly disappears in the parallel direction for $\lambda < 2$, as the inter-domain distance increases much more rapidly along the x-axis, while it remains almost constant in the transverse direction. Note that these very different behaviors between the two networks an important clue supporting the idea that the two hydrogels self-associate differently, even if they have the same average composition and share some close properties at low deformation.

In order to get additional information in the low intensity region, and more especially in the high *q*-range, the SANS data obtained with two neutron configurations were radially averaged along a given direction within a rectangular sector of axis parallel (//) or perpendicular (⊥), respectively, to the deformation axis. The corresponding intensities $I_{//}(q)$ and $I_{\perp}(q)$ are plotted respectively in **Figure 9** and **Figure S5** .

In the case of GPN-D (**Figures 9a** and **S5a**), the whole scattering spectra determined in the perpendicular direction remains almost unaffected by the deformation. The main difference arises at low *q* values where we simply observe a small decrease of the osmotic

compressibility that can be correlated to increasing repulsions between microdomains becoming closer. At large q values, the same interfaces are probed whatever the deformation is. The situation is very different in the stretching direction (//) as the Porod plots show that the q^{-4} dependence is shifted towards low q values with increasing deformation and that additional $q^{-\alpha}$ dependences appear at large q values with α ranging between 2 and 1; exponents corresponding to Gaussian or extended chains (see **Figure S6**). As this phenomenon occurs in the softening zone of the mechanical properties (i.e., above λ=2) it could be attributed to the stretching and unfolding of PNIPA chains within the polymer-rich phase as recently evoked by Sato et al. for hydrogels containing phase-separated polymer domains.[17] A similar scenario with domain distortion and splitting, initially proposed for GPD-N, can also be considered for GPN-D but as PNIPA chains now form the cross-linked backbone of the network, the deformation of bicontinuous microdomains should proceed differently.

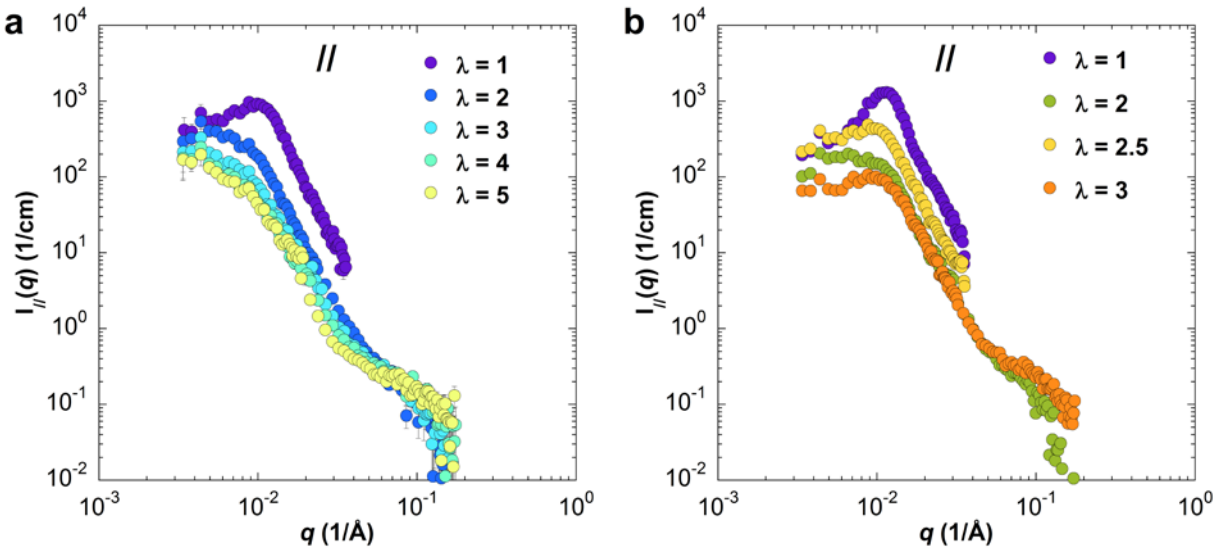

Figure 9. Scattered intensity profiles at 60 °C of hydrogels under uni-axial deformation. **a)** GPN-D (from λ = 1 to λ = 5) and **b)** GPD-N (from λ = 1 to λ = 3). The data were obtained from 2D-SANS after sector averaging in the parallel (//) direction of the deformation axis.

To support this discussion we can start from the theoretical works of Polotsky et al.[37] which describe the mechanical unfolding of a homopolymer globule. According to their self-consistent-field approach, the transition from the initial globular state to an extended conformation, above a critical deformation rate, is accompanied by an abrupt unfolding of the depleted globular head and a corresponding jump-wise drop in the intra-chain tension. It is worth noting that a similar macroscopic behavior has also been predicted a long time ago by Dušek and Patterson with stretched hydrogels in poor-solvent conditions.[38] If we transpose this concept of conformational transition to GPN-D, we can assume 1) that under weak deformation the microdomains will be gently elongated in the direction of stretching and compressed in the transverse direction and 2) that rapidly, above a given deformation threshold, domains will disrupt and "split" into dense regions connected by extended chains. This unfolding process with the formation of domains with stretched PNIPA chains can be supported by the asymptotic behavior observed in the parallel-direction as shown in **Figure 9a** and **Figure S6**. By comparison with the predictions of Polotsky et al.[37] the unfolding transition of PNIPA does not give rise to an abrupt drop of the internal stress of the network but the softening observed beyond $\lambda = 2$ in **Figure 7b** could be a signature of such process.

In the case of GPD-N (**Figure 9b** and **S5b**), the asymptotic behavior at large *q* has been studied only for two stretch ratios and it is more difficult to conclude with this system. Nevertheless we can see at $\lambda = 3$ some Porod's law with $\alpha \cong 2$ in agreement with a similar process of chain extension upon stretching.

Impact of network topology on fracture behavior.

With the micro-phase separation of PNIPA segments into polymer-rich domains, both hydrogels demonstrate qualitatively a large improvement of fracture resistance upon heating

beyond T_c (see **Figure 7b**). By introducing an initial edge notch on the gel, a clear distinction between toughening mechanisms at play in GPD-N and GPN-D topologies can be drawn. As shown in **Figure 10a**, the fracture resistance is greatly improved at 60 °C for both microphase-separated gels, but the thermo-toughening mechanisms operates differently for the two opposite gel topologies; the GPN-D structure with PNIPA forming the cross-linked network being more efficient and exhibiting a systematic crack bifurcation although the crack proceeds straightly in GPD-N. In the collapsed network GPN-D topology, the fibrillar collapsed PNIPA-rich domains (i.e. bearing the chemical cross-links), as schematically shown in **Figure 10b**, orient in the stretching direction especially in the vicinity of the crack tip where strain amplification is high. The structure is then similar to a laminate material where tough PNIPA-rich fibres are alternating with the PDMA swollen phase. As SANS experiments show that the average distance between PNIPA domains remains mostly unchanged in the transverse direction, this suggests that PNIPA-rich domains become thicker upon stretching. In these conditions, the crack will propagate more easily through the PDMA phase (i.e. in the direction of stretching) and then a crack deviation perpendicularly to the initial notch direction is induced. This mode of crack propagation involving deflection of the crack propagation direction is usually described as 'knotty tearing' and classically expected in natural rubbers,[39] but not in gels so far. By analogy with the natural rubber strain-crystallization, crack bifurcation in GPN-D gels may be directly related to the collapsed network topology. As reported previously,[20] there is a strong impact of the primary structure of GPN-D networks as the average molar mass of PNIPA sequences between PDMA side-chains, as well as the weight fraction of both polymers, control the characteristic length-scale of the phase separated morphology as the crack bifurcation process.

By comparison, the micellar morphology obtained with GPD-N (see **Figure 10b**) improves the overall mechanical properties by the introduction of physical cross-links at high

607 temperature but in this case crack proceeds straightly within the gel. The crack propagation
608 mechanisms of GPN-D and GPD-N are illustrated in **Figure S7** (see Supporting information)
609 with pictures taken at various strain levels.

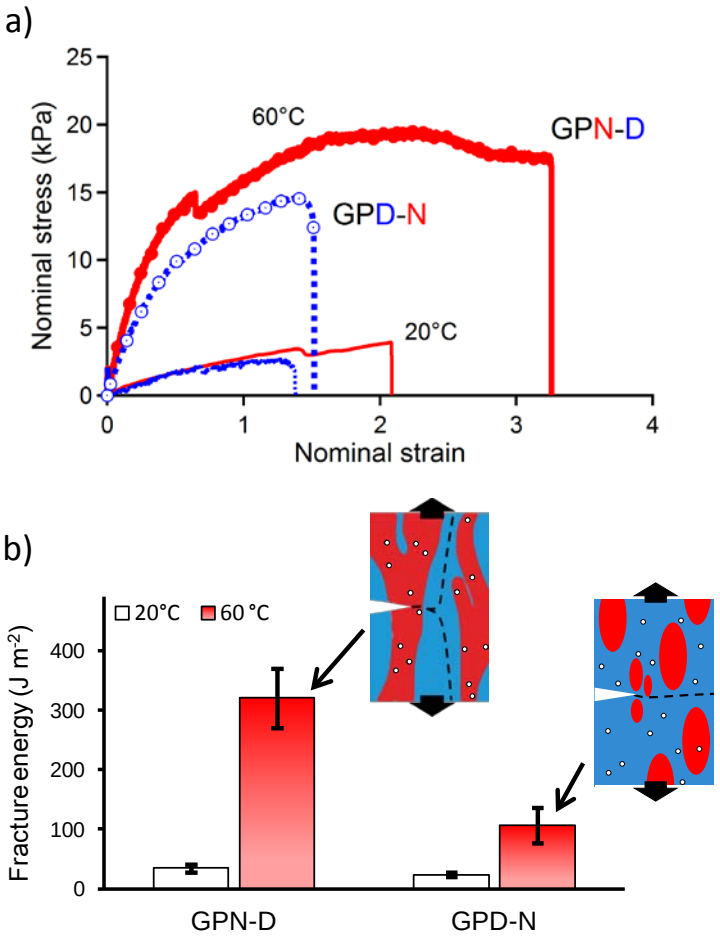

Figure 10. a) Fracture behavior of GPN-D (red continuous line) and GPD-N (blue dashed line) notched specimens at 20 and 60 °C and **b)** Fracture energies obtained at 20 and 60 °C. The scheme is a view of the reinforcing mechanisms at microscale. Dotted lines refer to damage mechanisms and define weak interfaces.

610
611 **Other route, other history.**

612 In previous experiments, 2D SANS were performed under deformation at 60 °C, starting from
613 an undeformed microphase separated sample. Interestingly, complementary information can

be obtained by changing the route, i.e. starting at 20 °C with a deformed sample (here λ=2) and then increasing the temperature to initiate the PNIPA phase separation in the deformed state. The 2D SANS spectra obtained from these two routes are compared in **Figures 11a** and **11b**. In the case of GPD-N, deformed below the phase transition, and heated up after deformation, the SANS pattern is almost isotropic with only a very weak prolate distorsion of 5 % in the perpendicular direction (**Figure 11a**). This result highlights that even in a stretched PDMA network, the PNIPA side chains self-associate with their surrounding neighbors forming isotropically distributed domains in good agreement with the micellar model and rather independently of the PDMA network stretching.

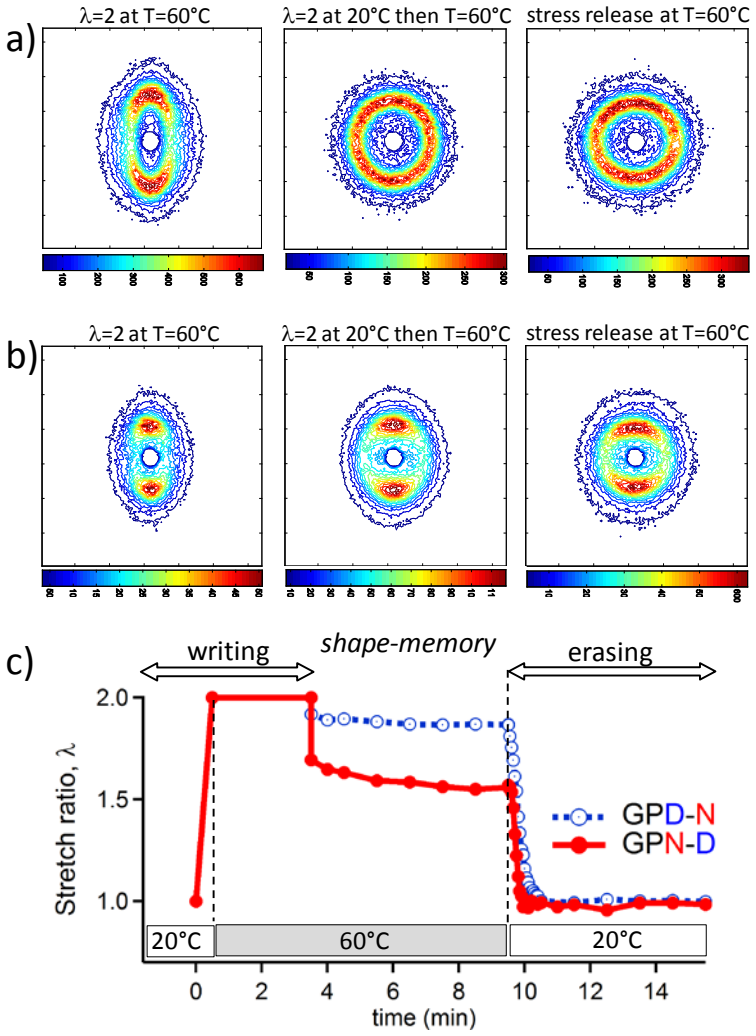

Figure 11. Shape memory behaviors of gels. Two-dimensional SANS images of a step-by-

step loading/heating process of **a)** GPD-N and **b)** GPN-D. The gels are heated at 60 °C prior to be deformed at λ=2 (left). The gels, initially deformed at λ=2 at 20 °C, are then heated at 60 °C (center). Then the stress of gels in the center is released at 60 °C (right): note that in these conditions the gels keep a residual strain to avoid buckling of the sample. The direction of the uni-axial deformation is along the horizontal axis. **c)** Shape recovery curves GPD-N (red continuous line) and GPN-D (blue dashed line) with time. First, the gels were stretched to λ=2 at 20 °C prior to be heated in oil at 60 °C to perform the "writing" procedure. After keeping λ=2 for 3 min at 60 °C, stress was released and the residual stretched ratio was measured over time. Finally, the gels were cooled at 20 °C to fulfill the "erasing" process.

The formation of concentrated aggregates, exhibiting slow dynamics as described previously, is also responsible for the shape memory effect as illustrated in **Figure 11c**. After "writing" a stretch level of λ=2 at 60 °C during 3 min, stress was removed with only a weak retraction of the structure. The stretch ratio is maintained overtime without significant relaxation processes. This result suggests that internal stresses due to the extension of the PDMA network are compensated by the formation of collapsed PNIPA microdomains that play the role of thermo-triggered cross-links. The dynamics of these physical cross-links is very slow down, otherwise the relaxation would have been much more important.

In the case of GPN-D, the difference between the two routes appears less pronounced as now the PNIPA backbone is topologically defined as the load bearing phase (**Figure 11b**). At 60 °C and λ=2, the two patterns are anisotropic. At macroscopic scale, as illustrated in **Figure 11c**, after removing the stress, the gel maintains its stretch level with a partial strain recovery (around 30%) and also slight relaxation processes..

This set of structural and mechanical analyzes clearly demonstrates that different morphologies with different mechanical properties can be obtained with the same topology according to the route of self-assembling. If the structure of PNIPA-rich domains is clearly

the central feature of the thermo-toughening mechanism, the dynamic properties of segregated PNIPA chains is an important characteristic to consider. According to the results obtained in this work it appears that phase separated PNIPA domains cannot be considered as frozen with the meaning of glassy (arrested phase) as they are able to respond elastically but the dynamics of exchange is intrinsically very slow and is responsible for the apparent stability of PNIPA-rich domains.

CONCLUSION

The original aim of this work was to investigate the effect of topology on thermo-toughening. Our original gel designs combine hydrophilic and LCST polymer chains within the same hydrogel in order to get thermo-responsive mechanical properties whilst avoiding the issue of the volume phase transition. This challenge was achieved successfully by playing with the network architecture and testing opposite topologies. Indeed, we show that graft hydrogels designed with the same PDMA/PNIPA composition (50/50), are able to develop responsive and reversible toughness with large enhancement of these properties by working under isochoric conditions. Nevertheless, the primary architecture is crucial, depending whether or not the responsive polymer belongs to the backbone.

When hydrogels are designed with a thermo-responsive PNIPA backbone, the phase transition occurs promptly above the critical temperature but PDMA side-chains allow to stabilize the phase separation at a microscopic level and to maintain a relative high level of swelling. Indeed, from DSC and SANS studies, GPN-D has been shown to respond with temperature with the formation of a bicontinuous structure which length scale grows with increasing temperature while remaining at a microscopic level. This gel shows remarkable responsive toughness with temperature and SANS clearly highlights that the distortion of the local

structure is non-affine with the network deformation. The responsive toughening of mechanical properties above the transition temperature can be attributed to the formation of a continuous rich-PNIPA phase that greatly enhances the energy dissipation within the hydrogel with in particular some original mechanism of crack bifurcation. This thermo-responsive enhancement of the mechanical properties can be compared with recent results reported by Gong et al.[17] in the case of polyacrylamide gels where toughening was induced by phase separation in water/organic solvent mixtures. Taking into account the literature background related to the stretching of single globular chain or polymer network in bad solvent, we propose that under stretching the PNIPA domains start to deform and give rise to yielding with chain extension and unfolding. On the contrary, when hydrogels are designed with PNIPA side-chains, these latter self-assemble above the transition temperature forming a micellar network with a fairly high polymer concentration inside the core (~ 75%). The transition temperature is a little bit higher for these systems because they are attached to the PDMA backbone with no direct neighbors. The very low dissociation rate of PNIPA chains from aggregates at high temperature is responsible for their frozen-like morphologies. This aspect was highlighted macroscopically with shape memory experiments, and locally as well with SANS patterns obtained by following different routes. Even if the covalent cross-links which belong to the PDMA frame are located outside the PNIPA cores, the rheology and tensile tests suggest a strong coupling between covalent and physical cross-links as the elastic modulus is very close for both GPD-N and GPN-D. Nevertheless, fracture experiments performed on notched samples have shown that the micellar organization of PNIPA domains in GPD-N is less effective to reduce the fracture propagation. The micellar morphology of GPD-N displays common features with hybrid hydrogels which are prepared by dispersing silica nanoparticles in a PDMA network for similar polymer composition.[23] Indeed, in this case, the reinforcement arises from a strong coupling between the covalent PDMA network

and the specific interactions taking place between silica surfaces and PDMA chains. One of the main differences is that nanoparticles are non-deformable, while in GPD-N gels, PNIPA spherical domains can be distorted in the direction of deformation and split for large deformation.

The main conclusion of this work is that the LCST-type phase transition can be readily used as a trigger to strongly and reversibly enhance the mechanical properties of hydrogels; their swelling ability being retained at high temperature by the hydrophilic counterpart. The phase separated structure is strongly correlated to the initial network architecture and the introduction of PNIPA within the backbone provides the best coupling between physical and covalent cross-links. Not only the structure but also the scale of the phase separation is a critical parameter to control the mechanical properties. These considerations pave the way for new ideas concerning the structure/properties relationships in responsive toughening of hydrogels with applications in biomedicine and other industrial fields.

ACKNOWLEDGEMENTS

We gratefully acknowledge the financial support of CNRS, ESPCI and UPMC and the China Scholarship Council for the PhD fellowship funding of Hui Guo. The authors also thank Guylaine Ducouret from SIMM for technical advice on performing rheological measurements and François Boué from Agro ParisTech for helpful discussions on neutron scattering experiments.

REFERENCES

1. Peppas, N. A., *Hydrogels in medicine and pharmacy*, CRC press Boca Raton, FL: 1987; Vol. 3.
2. Buchholz, F. L. G., A. T. *Modern Superabsorbent Polymer Technology; Wiley-VCH: New-York* **1997**.
3. Hoare, T. R.; Kohane, D. S. Hydrogels in drug delivery: progress and challenges. *Polymer* **2008**, *49*, 1993-2007.
4. Oh, J. K.; Drumright, R.; Siegwart, D. J.; Matyjaszewski, K. The development of microgels/nanogels for drug delivery applications. *Prog. Polym. Sci.* **2008**, *33*, 448-477.
5. Gong, J. P.; Katsuyama, Y.; Kurokawa, T.; Osada, Y. Double-network hydrogels with extremely high mechanical strength. *Adv. Mater.* **2003**, *15*, 1155-1158.
6. Okumura, Y.; Ito, K. The polyrotaxane gel: A topological gel by figure of eight cross-links. *Adv. Mater.* **2001**, *13*, 485-487.
7. Matsunaga, T.; Sakai, T.; Akagi, Y.; Chung, U.-i.; Shibayama, M. SANS and SLS studies on tetra-arm PEG gels in as-prepared and swollen states. *Macromolecules* **2009**, *42*, 6245-6252.
8. Haraguchi, K.; Takehisa, T.; Fan, S. Effects of clay content on the properties of nanocomposite hydrogels composed of poly (N-isopropylacrylamide) and clay. *Macromolecules* **2002**, *35*, 10162-10171.
9. Carlsson, L.; Rose, S.; Hourdet, D.; Marcellan, A. Nano-hybrid self-crosslinked PDMA/silica hydrogels. *Soft Matter* **2010**, *6*, 3619-3631.
10. Abdurrahmanoglu, S.; Can, V.; Okay, O. Design of high-toughness polyacrylamide hydrogels by hydrophobic modification. *Polymer* **2009**, *50*, 5449-5455.
11. Henderson, K. J.; Zhou, T. C.; Otim, K. J.; Shull, K. R. Ionically cross-linked triblock copolymer hydrogels with high strength. *Macromolecules* **2010**, *43*, 6193-6201.
12. Hao, J.; Weiss, R. Viscoelastic and mechanical behavior of hydrophobically modified hydrogels. *Macromolecules* **2011**, *44*, 9390-9398.
13. Sun, J.-Y.; Zhao, X.; Illeperuma, W. R.; Chaudhuri, O.; Oh, K. H.; Mooney, D. J.; Vlassak, J. J.; Suo, Z. Highly stretchable and tough hydrogels. *Nature* **2012**, *489*, 133-136.

14. Sun, T. L.; Kurokawa, T.; Kuroda, S.; Ihsan, A. B.; Akasaki, T.; Sato, K.; Haque, M. A.; Nakajima, T.; Gong, J. P. Physical hydrogels composed of polyampholytes demonstrate high toughness and viscoelasticity. *Nat. Mater.* **2013**, *12*, 932-937.

15. Tanaka, T. Phase transitions in gels and a single polymer. *Polymer* **1979**, *20*, 1404-1412.

16. Shibayama, M.; Morimoto, M.; Nomura, S. Phase separation induced mechanical transition of poly (N-isopropylacrylamide)/water isochore gels. *Macromolecules* **1994**, *27*, 5060-5066.

17. Sato, K.; Nakajima, T.; Hisamatsu, T.; Nonoyama, T.; Kurokawa, T.; Gong, J. P. Phase-Separation-Induced Anomalous Stiffening, Toughening, and Self-Healing of Polyacrylamide Gels. *Adv. Mater.* **2015**, *27*, 6990-6998.

18. Kamata, H.; Akagi, Y.; Kayasuga-Kariya, Y.; Chung, U.-i.; Sakai, T. "Nonswellable" hydrogel without mechanical hysteresis. *Science* **2014**, *343*, 873-875.

19. Muniz, E. C.; Geuskens, G. Compressive elastic modulus of polyacrylamide hydrogels and semi-IPNs with poly (N-isopropylacrylamide). *Macromolecules* **2001**, *34*, 4480-4484.

20. Guo, H.; Sanson, N.; Hourdet, D.; Marcellan, A. Phase-separated hydrogels under isochoric conditions display thermo-responsive toughening with crack bifurcation. *Adv. Mater.* **2016**. DOI: 10.1002/adma.201600514.

21. Guo, H.; Brûlet, A.; Rajamohanan, P. R.; Marcellan, A.; Sanson, N.; Hourdet, D. Influence of topology of LCST-based graft copolymers on responsive assembling in aqueous media. *Polymer* **2015**, *60*, 164-175.

22. Greensmith, H. Rupture of rubber. X. The change in stored energy on making a small cut in a test piece held in simple extension. *J. Appl. Polym. Sci.* **1963**, *7*, 993-1002.

23. Rose, S.; Marcellan, A.; Narita, T.; Boué, F.; Cousin, F.; Hourdet, D. Structure investigation of nanohybrid PDMA/silica hydrogels at rest and under uniaxial deformation. *Soft Matter* **2015**, *11*, 5905-5917.

24. Shibayama, M.; Tanaka, T.; Han, C. C. Small-angle neutron scattering study on weakly charged temperature sensitive polymer gels. *J. Chem. Phys.* **1992**, *97*, 6842-6854.

25. Shibayama, M.; Kurokawa, H.; Nomura, S.; Roy, S.; Stein, R. S.; Wu, W. L. Small-angle neutron scattering studies on chain asymmetry of coextruded poly (vinyl alcohol) film. *Macromolecules* **1990**, *23*, 1438-1443.

26. Teubner, M.; Strey, R. Origin of the scattering peak in microemulsions. *J. Chem. Phys.* **1987**, *87*, 3195-3200.

27. László, K.; Kosik, K.; Geissler, E. High-sensitivity isothermal and scanning microcalorimetry in PNIPA hydrogels around the volume phase transition. *Macromolecules* **2004**, *37*, 10067-10072.

28. Bastide, J.; Leibler, L. Large-scale heterogeneities in randomly cross-linked networks. *Macromolecules* **1988**, *21*, 2647-2649.

29. Karino, T.; Okumura, Y.; Zhao, C.; Kataoka, T.; Ito, K.; Shibayama, M. SANS studies on deformation mechanism of slide-ring gel. *Macromolecules* **2005**, *38*, 6161-6167.

30. Mendes, E.; Oeser, R.; Hayes, C.; Boue, F.; Bastide, J. Small-angle neutron scattering study of swollen elongated gels: butterfly patterns. *Macromolecules* **1996**, *29*, 5574-5584.

31. Shibayama, M.; Kawakubo, K.; Ikkai, F.; Imai, M. Small-angle neutron scattering study on charged gels in deformed state. *Macromolecules* **1998**, *31*, 2586-2592.

32. Shibayama, M. Small-angle neutron scattering on polymer gels: phase behavior, inhomogeneities and deformation mechanisms. *Polym. J.* **2011**, *43*, 18-34.

33. Reynders, K.; Mischenko, N.; Mortensen, K.; Overbergh, N.; Reynaers, H. Stretching-induced correlations in triblock copolymer gels as observed by small-angle neutron scattering. *Macromolecules* **1995**, *28*, 8699-8701.

34. Rharbi, Y.; Cabane, B.; Vacher, A.; Joanicot, M.; Boué, F. Modes of deformation in a soft/hard nanocomposite: A SANS study. *EPL (Europhysics Letters)* **1999**, *46*, 472-478.

35. Ikeda, Y.; Yasuda, Y.; Yamamoto, S.; Morita, Y. Study on two-dimensional small-angle X-ray scattering of in situ silica filled nanocomposite elastomer during deformation. *J. Appl. Crystallogr.* **2007**, *40*, 549-552.

36. Nishida, T.; Endo, H.; Osaka, N.; Li, H.-j.; Haraguchi, K.; Shibayama, M. Deformation mechanism of nanocomposite gels studied by contrast variation small-angle neutron scattering. *Phys. Rev. E* **2009**, *80*, 030801.1-030801.4.

37. Polotsky, A. A.; Charlaganov, M. I.; Leermakers, F. A.; Daoud, M.; Borisov, O. V.; Birshtein, T. M. Mechanical unfolding of a homopolymer globule studied by self-consistent field modeling. *Macromolecules* **2009**, *42*, 5360-5371.

38. Dušek, K.; Patterson, D. Transition in swollen polymer networks induced by intramolecular condensation. *J. Polym. Sci. Pol. Chem.* **1968**, *6*, 1209-1216.

39. Hamed, G. R. Molecular aspects of the fatigue and fracture of rubber. *Rubber Chem. Technol.* **1994**, *67*, 529-536.

"For Table of Contents use only"

Thermo-responsive Toughening in LCST-type Hydrogels with Opposite Topology: From Structure to Fracture Properties.

Hui Guo, Cécile Mussault, Annie Brûlet, Alba Marcellan,* Dominique Hourdet,* and Nicolas Sanson*